Clinical and Experimental Obstetrics & Gynecology

Clin. Exp. Obstet. Gynecol. **2025**; 52(12): 45103
https://doi.org/10.31083/CEOG45103

Case Report

Cervical SMARCA4-Deficient Undifferentiated Tumor: A Rare Case Report and Literature Review

Jin Wang[1], Yanli Li[2], Wanhui Dong[3], Chuanying Li[4,*]

[1]Department of Pathology, Affiliated Hospital of West Anhui Health Vocational College, 237000 Liu'an, Anhui, China
[2]Department of Pathology, School of Basic Medical Sciences, Anhui Medical University, 230001 Hefei, Anhui, China
[3]Department of Medical Oncology, Liu'an Hospital of Traditional Chinese Medicine, 237000 Liu'an, Anhui, China
[4]Department of Pathology, Ruijin Hospital, Affiliated with Shanghai Jiao Tong University School of Medicine, 200025 Shanghai, China
*Correspondence: lcy12224@rjh.com.cn (Chuanying Li)
Academic Editor: Michael H. Dahan
Submitted: 18 July 2025 Revised: 17 September 2025 Accepted: 26 September 2025 Published: 22 December 2025

Abstract

Background: The cervical switch (SWI)/sucrose non-fermentable (SNF) related, matrix associated, actin dependent regulator of chromatin, subfamily a, member 4 (*SMARCA4*)-deficient undifferentiated tumor (*SMARCA4*-UT) constitutes a rare, highly aggressive malignancy that is currently unclassified by the World Health Organization (WHO). The published literature comprises predominantly sporadic case reports. Clinically characterized by an unfavorable prognosis, distinctive histopathological morphology, and specific immunophenotypic profiles, a cervical *SMARCA4*-UT exhibits relatively nonspecific molecular alterations that closely mirror those of a thoracic *SMARCA4*-UT. Notably, optimal therapeutic algorithms and management paradigms remain incompletely delineated. **Case**: We report a case of cervical *SMARCA4*-UT in a 58-year-old female presenting with persistent abnormal uterine bleeding. The initial clinical evaluation, including ultrasonography, identified a cervical mass. The patient was subsequently referred to a hospital. Comprehensive staging, using whole-body positron emission tomography-computed tomography (PET-CT) and pelvic magnetic resonance imaging (MRI), confirmed a large cervical neoplasm consistent with clinical stage IV disease, precluding radical surgical resection. Analysis of biopsy specimens demonstrated partial pan-cytokeratin [anti-epithelial cytokeratin 1 (AE1)/anti-epithelial cytokeratin 3 (AE3)] immunoreactivity, focal claudin-4 expression, and complete loss of SMARCA4 protein expression. Next-generation sequencing (NGS) identified a microsatellite instability-high (MSI-H) status, with mutations in genes such as phosphatase and tensin homolog deleted on chromosome ten (*PTEN*) and AT-rich interaction domain 1A (*ARID1A*), among others; notably, pathogenic *SMARCA4* mutations were absent. A definitive diagnosis of *SMARCA4*-UT was established. Therapeutic intervention comprised percutaneous radioactive seed implantation followed by combination chemotherapy with etoposide-cisplatin (EP regimen) plus bevacizumab, complicated by bone marrow suppression. Therapy was transitioned to pembrolizumab combined with paclitaxel-carboplatin (TP regimen). Disease progression prompted the reversion to a reduced EP regimen with bevacizumab dosage. The patient demonstrated sustained disease control from her third discharge until the conclusion of the follow-up. **Conclusions**: Single-agent immunotherapy has shown limited efficacy in the inoperable setting, whereas combination chemotherapy regimens incorporating anti-vascular endothelial growth factor (VEGF) agents may have conferred a clinical benefit for tumor control.

Keywords: cervical cancer; immunotherapy; pathological diagnosis; prognosis; *SMARCA4*-deficient tumor

1. Introduction

Switch (SWI)/sucrose non-fermentable (SNF) related, matrix associated, actin dependent regulator of chromatin, subfamily a, member 4 (*SMARCA4*)-deficient undifferentiated tumor (*SMARCA4*-UT) tumors were newly recognized as a distinct entity in the 2021 World Health Organization (WHO) Classification of Thoracic Tumors. These tumors are characterized by the loss of SMARCA4 tumor suppressor protein expression and predominantly arise in the anterior mediastinum. Patients diagnosed with *SMARCA4*-UT tumors have a median survival of approximately seven months [1]. Furthermore, *SMARCA4* gene alterations have been implicated in various malignancies, including those of the central nervous system, head and neck, gastrointestinal tract, urogenital tract, soft tissues, and thoracic region. Although rare, there have been sporadic case reports describing *SMARCA4*-UT tumors occurring in the cervix [2,3]. Notably, the most recent edition of the WHO Classification of Tumors of the Female Reproductive Tract did not include specific descriptions or classifications for *SMARCA4*-deficient undifferentiated cervical tumors. Furthermore, *SMARCA4* deletion in most such tumors is confined to the protein level and remains undetected by next-generation sequencing (NGS), presenting significant diagnostic challenges for cervical *SMARCA4*-UTs. Given the markedly poor clinical prognosis and short survival periods associated with *SMARCA4*-UT, formulating effective treatment strategies has therefore become particularly urgent.

The present case study delineated a case of *SMARCA4*-UT, detailing its histological characteristics. Immunohistochemical analysis demonstrated positive

anti-epithelial cytokeratin 1 (AE1)/anti-epithelial cytokeratin 3 (AE3) staining in distinct regions, focal Claudin-4 positivity, and complete absence of SMARCA4 protein expression. The differential diagnostic considerations and investigative approach are discussed. Additional genetic variants identified via NGS potentially expand the genotypic spectrum associated with this unique patient population. Therapeutic strategies were evaluated; immunotherapy demonstrated limited efficacy in this tumor subtype. However, chemotherapy combined with anti-vascular endothelial growth factor (VEGF) agents exhibited potential for inhibiting tumor growth, suggesting new therapeutic promise for this category of malignancies.

2. Case Presentation

The patient was a 58-year-old woman who experienced menarche at the age of 13, which is within the normal physiological range. She had regular menstrual cycles with moderate flow and experienced varying degrees of dysmenorrhea during menstruation. On December 16, 2024, the patient presented with abnormal menstruation, characterized by persistent dark-red vaginal bleeding accompanied by a small amount of abnormal vaginal discharge. Throughout this period, there were no obvious abdominal discomforts, such as abdominal pain or bloating. After medical consultation at a local hospital, detailed physical examination and gynecological ultrasound suggested possible cervical tumor lesions. Although initial pharmacological treatment resulted in partial control of vaginal bleeding, follow-up assessments showed no significant change in tumor size. As her condition progressed, she gradually developed new symptoms, including lower abdominal distension and intermittent dull pain.

The patient was referred to Ruijin Hospital, affiliated with Shanghai Jiao Tong University School of Medicine, on January 22, 2025, for further specialized diagnosis and management. Comprehensive positron emission tomography-computed tomography (PET-CT) whole-body imaging and pelvic magnetic resonance imaging (MRI) (specific findings shown in Fig. 1) revealed a bulky cervical tumor. Based on the International Federation of Gynecology and Obstetrics (FIGO) staging system, the tumor was clinically staged as stage IV.

Owing to the extensive tumor volume, the patient was deemed ineligible for radical surgical resection and subsequently underwent biopsy of a limited tumor tissue specimen for histopathological analysis. In this case, the limited quantity of biopsy tissues posed a significant challenge. Moreover, within the framework of the existing WHO classification for the female reproductive system, there had been no reported description of a similar case, and currently, case reports on this condition are scarce. The non-specific molecular characteristics further compounded the diagnostic difficulty. Given these circumstances, accurate diagnosis of this case was difficult.

The specimen sent to the pathology department consisted of fragmented grayish—brown tissue clumps with a volume of 2.0 $\times$ 2.0 $\times$ 1.0 cm. Hematoxylin and eosin (H&E) sections demonstrated an infiltrative neoplasm with solid, sheet-like growth and heterogeneous cellular density. Perivascular invasion and extensive necrosis were evident (Fig. 2A,B). High-power examination revealed monomorphic tumor cells exhibiting vesicular nuclei with hyperchromasia, prominent nucleoli, and eosinophilic cytoplasm. Rhabdoid morphology predominated (Fig. 2C), featuring eccentric nuclei, marked atypia, and readily identifiable mitoses in hyperchromatic cells. Stroma showed minimal inflammation with focal myxoid matrix (Fig. 2D).

During the pathological diagnostic process, we distinguished four distinct entities: (1) *SMARCA4*-deficient uterine sarcoma (SDUS); (2) Undifferentiated endometrial carcinoma (UDEC); (3) Ovarian hypercalcemic small cell carcinoma (SCCOHT); and (4) Conventional cervical carcinoma. Key differential diagnostic criteria comprised: (a) Imaging findings demonstrating a large cervical mass, effectively excluding SCCOHT as it represents a highly malignant ovarian tumor; (b) Immunohistochemical (Fig. 3 shows some of the immunohistochemical results) analysis revealing partial AE1/AE3 positivity, focal Claudin-4 immunoreactivity, complete loss of SMARCA4 protein expression, patchy p16 positivity, and tumor protein p53 (p53) positivity in 90% of tumor cells. SDUS characteristically exhibits negative Claudin-4 staining. The absence of SMARCA4 protein expression excluded conventional cervical carcinoma. In UDEC, approximately 34% of cases harbor tumor protein 53 (*TP53*) mutations and about 44% demonstrate microsatellite instability (MSI) [4], thereby differentiating it from SDUS. The H&E morphology of UDEC, featuring undifferentiated carcinoma or rhabdomyoid cells, resembled the current case. Immunohistochemical analysis similarly showed loss of SMARCA4 expression, AE1/AE3 positivity, Claudin-4 positivity, and p53 mutation. Nevertheless, differentiation from the present case remained challenging. In contrast, the primary lesion in this case was cervical in origin and demonstrated patchy p16 positivity (NOTE: Based on the experimental protocol, immunohistochemical staining was performed using the EnVision™ FLEX detection system (Standard, Dako/Agilent, Santa Clara, CA, USA, Cat. K8000; Patent EP1301268B1). Primary antibodies against SMARCA4 (rabbit monoclonal, clone EP235; dilution 1:150), pan-cytokeratin AE1/AE3 (mouse monoclonal, clone AE1/AE3-P; dilution 1:80), P16INK4a (mouse monoclonal, clone E6H4; dilution 1:1), TP53 (mouse monoclonal, clone DO-7; dilution 1:100) and CLDN4 (Claudin-4) (Rabbit monoclonal, clone EP145; dilution 1:200) were procured from Leica Biosystems (Leica Biosystems GmbH, Am Lustbühel 1, 69126 Heidelberg, Baden-Württemberg, Germany) and Agilent Dako (Dako Denmark A/S, Produktionsvej 42, 2600 Glostrup, Denmark), respectively. Based

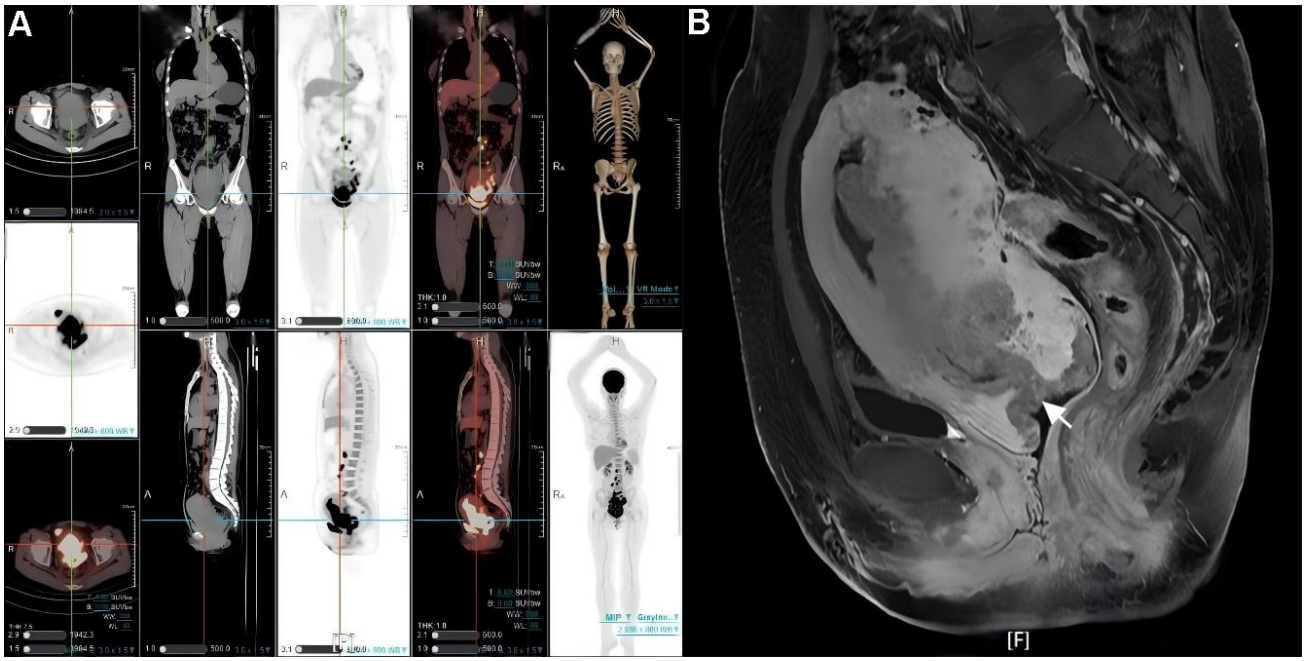

Fig. 1. PET-CT and MRI show the location of the tumor. Imaging findings demonstrated an irregular hypodense cervical lesion that extends superiorly into the uterine corpus and inferiorly involves the vaginal canal demonstrated by (A) PET-CT imaging and (B) pelvic MRI (The arrow designates a substantial mass lesion occupying the endocervical canal). PET-CT, positron emission tomography-computed tomography; MRI, magnetic resonance imaging.

on these collective findings, the diagnosis was more consistent with a cervical *SMARCA4*-UT. Paraffin-embedded tissue samples were subjected to NGS, which revealed microsatellite instability-high (MSI-H) status and identified 12 distinct mutations across 688 tumor-related genes (results detailed in Table 1) [NOTE: The NGS reagents (Cat. No. SH-SEQ2025) were procured from Shihuo Biotech Co., Ltd. (Shanghai, China), and all experimental procedures, including library preparation and sequencing runs, were conducted in strict accordance with the manufacturer's protocol (Version 3.1, issued 2024)].

On January 24, 2025, the patient underwent Implantable Venous Access Port (IVAP), followed by EP (cisplatin 75 mg/m^2 d1, etoposide 100 mg/m^2 d1–3) chemotherapy, combined with bevacizumab (15 mg/kg d1, q3w). However, significant myelosuppression occurred after treatment initiation, necessitating a switch to TP (T = 135 mg/m^2, P = 50 mg/m^2 d2) chemotherapy. Because of the MSI-H status that was detected by NGS, pembrolizumab (200 mg d1) was added to the therapeutic regimen. Nevertheless, imaging performed in March demonstrated tumor progression with increased volume, prompting modification of the treatment plan to reduced-dose EP chemotherapy while continuing bevacizumab therapy. From the third discharge in March 2025 until the most recent follow-up, the patient's general condition remained stable, and she is currently surviving with tumor-bearing status.

3. Discussion

Brahma-related gene 1 (*BRG1*, *SMARCA4*) and Brahma homolog (*BRM*, *SMARCA2*), as the catalytic subunits of the mammalian switch/sucrose non-fermentable Chromatin Remodeling Complex (mSWI/SNF or BAF) complex, are highly evolutionarily conserved. This complex plays a central role in chromatin remodeling [5]. It regulates transcription by altering nucleosome topology through adenosine triphosphate (ATP)-dependent mechanisms. Cancer genomic study has revealed that more than 20% of human tumors harbor mutations in one or more components of the BAF complex [6]. Experimental evidence has demonstrated that most of these mutations contribute to increased tumorigenesis, supporting the tumor-suppressive function of the BAF complex under normal physiological conditions [7].

SMARCA4 (*BRG1*), as the ATPase core of the complex, provides the enzymatic driving force [8] and is therefore also recognized as a tumor suppressor. It encodes the BRG1 protein, which forms functional complexes essential for chromatin regulation. Moreover, *SMARCA4* is among the most frequently mutated chromatin remodeling ATPases in cancer, accounting for approximately 5–7% of all human malignancies, with mutations predominantly located in evolutionarily conserved ATPase domains [9]. In a cohort study of *SMARCA4*-deficient non-small cell lung cancer (*SMARCA4*-dNSCLC), recurrent somatic mutations were identified in genes including *SMARCA4*, *KRAS*, and *TP53* [10]. Notably, patients harboring alter-

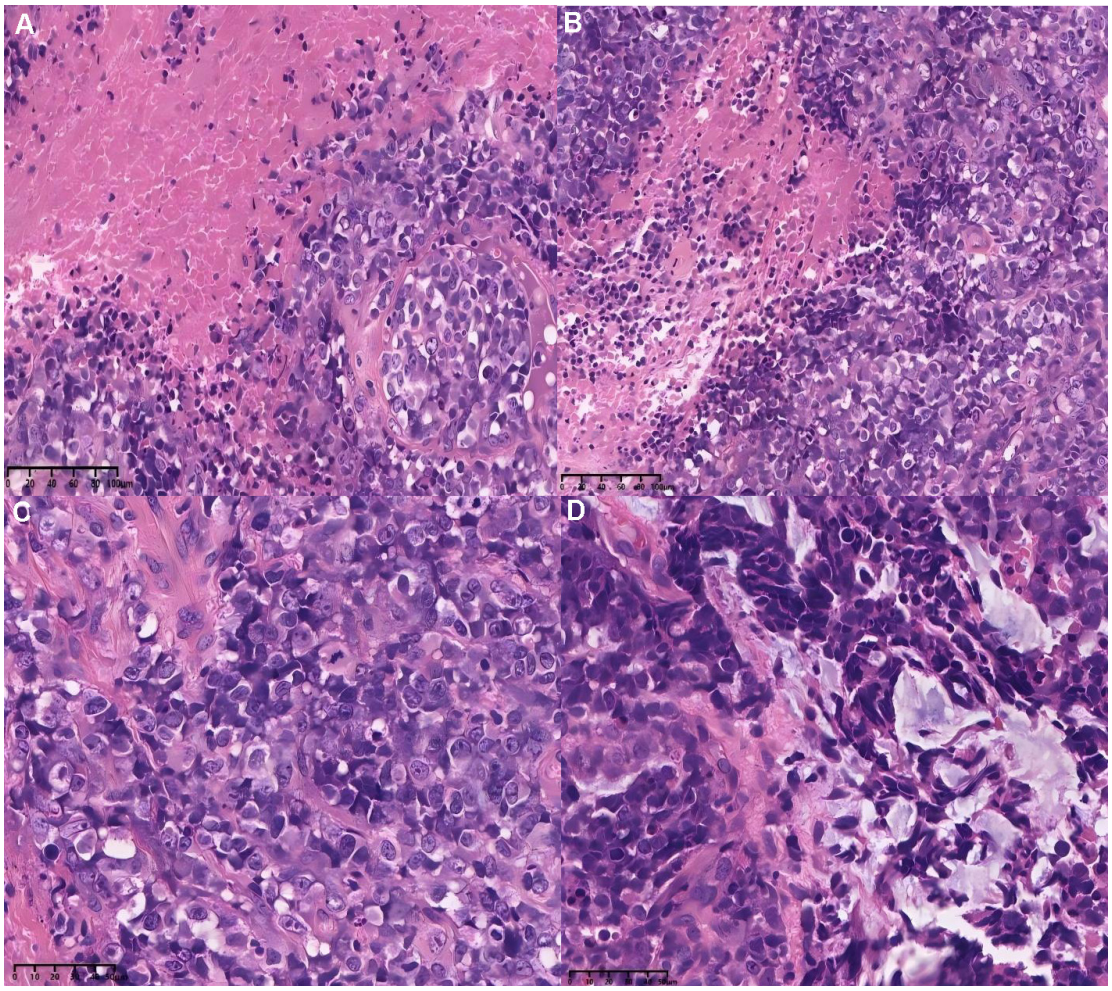

Fig. 2. Hematoxylin and eosin (H&E) staining (20×) demonstrated two characteristic histopathological features. (A) Perivascular invasion with neoplastic cells encircling and infiltrating vascular channels (*in situ* angioinvasion). Scale bar: 100 µm. (B) Extensive geographic zones of coagulative necrosis occupying approximately 30% of the tumor bulk. A high-power view (20×) (Scale bar: 100 µm) illustrated the following features: (C) Neoplastic cells exhibiting distinctive cytomorphology, characterized by eccentrically located ovoid nuclei with vesicular chromatin, observable nuclear fragmentation, and prominent eosinophilic paranuclear cytoplasmic inclusions; and focal rhabdoid features marked by cytoplasmic globular inclusions (40×). Scale bar: 50 µm. (D) The tumor stroma contained scattered inflammatory cells, with focal areas exhibiting an associated myxoid matrix (40×). Scale bar: 50 µm.

ations in *SMARCA4*, *TP53*, or serine/threonine kinase 11 (*STK11*) exhibited significantly shortened median overall survival compared to those without these genetic alterations [11].

SMARCA4 variations comprise two primary categories: Type I includes truncating mutations, gene fusions, and homozygous deletions, which result in complete loss of function; Type II comprises missense mutations that may exert dominant-negative or gain-of-function effects, either with or without functional loss [12]. An experimental study has demonstrated a high degree of consistency between the proportion of *SMARCA4*-subunit deletions and *SMARCA4*-gene mutations [13], leading researchers to suggest that genetic mutations may be the primary cause of protein expression loss. However, NGS has revealed that *SMARCA4* gene mutations do not necessarily result in protein deficiency. For instance, missense mutations and allele mutations have been observed without corresponding protein expression loss [14], indicating that molecular sequencing is not essential for diagnosing *SMARCA4*-deficient tumors. Currently, the absence of SMARCA4 (BRG1) protein expression is widely used as a diagnostic marker for *SMARCA4*-UT.

Therefore, in clinical settings, immunohistochemical confirmation of SMARCA4 protein loss, as observed in this case, may be sufficient for diagnosis, particularly when NGS fails to detect typical *SMARCA4* gene variants. According to recent data from The Cancer Genome Atlas (TCGA) [15,16], such cases account for approximately 15–20% of *SMARCA4*-UT diagnoses.

The present case results were identified through NGS, which revealed an AT-rich interaction domain 1A (*ARID1A*) gene mutation. As the largest subunit of the BAF com-

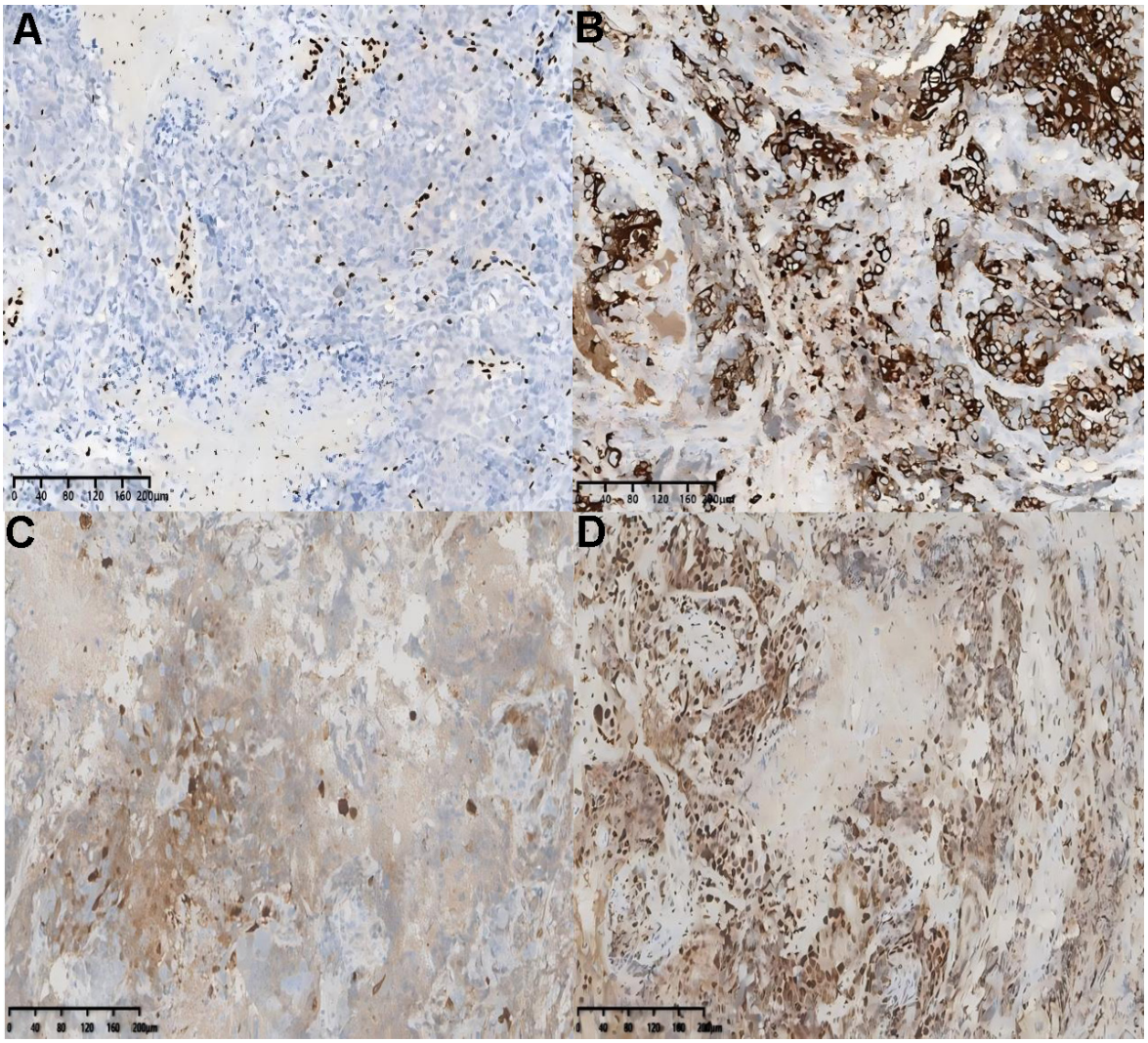

Fig. 3. Display immunohistochemical (IHC) images demonstrating tumor-specific diagnostic markers. IHC analysis (10×) revealed (A) a complete loss of nuclear SMARCA4 expression in neoplastic cells. Assessment of epithelial differentiation (10×) (Scale bar: 200 µm) demonstrated the following: (B) Focal cytoplasmic reactivity for AE1/AE3 in less than 30% of tumor cells (Scale bar: 200 µm). (C) The epidermis exhibited variable p16 staining intensity (10×) (Scale bar: 200 µm). (D) Tumor cells demonstrated a 90% cellular tumor antigen p53 (p53) positivity rate (10×) (Scale bar: 200 µm). SMARCA4, switch (SWI)/sucrose non-fermentable (SNF) related, matrix associated, actin dependent regulator of chromatin, subfamily a, member 4; AE1, anti-epithelial cytokeratin 1; AE3, anti-epithelial cytokeratin 3.

plex [17], *ARID1A* is characterized by frequent mutations across diverse human malignancies. These mutations impair the chromatin remodeling function of the complex, thereby promoting tumor-cell proliferation and invasiveness. Furthermore, by disrupting cell cycle regulatory pathways, these mutations drive aberrant cell proliferation [18]. A study reveals that the *ARID1A*-containing SWI/SNF complex (*ARID1A/SWI/SNF*) serves as a potent inhibitor of the pro-oncogenic transcriptional coactivators yes-associated protein (*YAP*) and transcriptional coactivator with PDZ-binding motif (*TAZ*), effectively suppressing their activity and thereby curbing uncontrolled cell proliferation and tumor formation [19]. Evidence has confirmed that *SMARCA4* deficiency frequently coexists with *ARID1A* mutations, and their concurrent occurrence in lung cancer may impair transcriptional regulation [20]. This may have accounted for the observed reduction in SMARCA4 protein expression despite the absence of detectable gene deletions. An alternative explanation involves limitations inherent in current detection methods: NGS technology exhibits restricted coverage for specific mutation classes, potentially leading to the oversight of pathogenic variants affecting *SMARCA4*.

SMARCA4-UT was first described in 2015 as a group of undifferentiated thoracic malignant neoplasms [21]. Initially classified as a sarcoma-like tumor, accumulating molecular evidence has led to its reclassification as a dedifferentiated or undifferentiated carcinoma [22]. Conse-

Table 1. The prominent genomic variants detected by next-generation sequencing (NGS).

Gene	Mutation type	Exon	cDNA	Amino acid alteration	Abundance
PTEN	Missense	exon5	c.T323C	p.L108P	59.99%
PIK3CA	Missense	exon21	c.C3139T	p.H1047Y	30.62%
KRAS	Missense	exon2	c.G35T	p.G12V	29.06%
ARID1A	Frameshift	exon12	c.3344delC	p.P1115Qfs*46	28.62%
CFTR	Frameshift	exon14	c.2089delA	p.R697Gfs*25	27.65%
MYC	Missense	exon3	c.A1121G	p.H374R	60.07%
BCOR	Missense	exon10	c.A4376G	p.N1459S	30.78%
CCND1	Insertion	exon5	c.866_877del	p.D289_D292del	29.80%
LRP1B	Missense	exon49	c.G7924T	p.G2642W	29.51%
ZNRF3	Missense	exon7	c.C1000T	p.R334W	29.34%
NOTCH3	Missense	exon31	c.G5705A	p.R1902H	28.80%
MUC16	Missense	exon50	c.G40124A	p.C13375Y	27.58%

PTEN, phosphatase and tensin homolog deleted on chromosome ten; *PIK3CA*, phosphoinositide-3-kinase catalytic subunit alpha; *KRAS*, Kirsten rat sarcoma viral oncogene homolog; *ARID1A*, AT-rich interaction domain 1A; *CFTR*, cystic fibrosis transmembrane conductance regulator; *MYC*, myelocytomatosis oncogene; *BCOR*, BCL6 corepressor; *CCND1*, cyclin D1; *LRP1B*, low-density lipoprotein receptor-related protein 1B; *ZNRF3*, zinc and ring finger 3; *NOTCH3*, Notch receptor 3; *MUC16*, Mucin 16.

quently, the WHO classification (5th Ed.) categorizes this entity under "other epithelial tumors". *SMARCA4*-UT is a high-grade malignancy characterized by an undifferentiated or rhabdoid morphology and the absence of SMARCA4 expression [23]. A recent study has indicated that *SMARCA4*-UT can occur across multiple anatomical sites beyond the thorax, including the lung [24], gallbladder [25], paranasal sinuses [26], nasopharynx [27], gastrointestinal tract [28–31], adrenal gland [31], urothelium [32], and skin [33].

As of 2020, the WHO classification of tumors of the female genital tract did not specifically describe *SMARCA4*-UT [34]. However, that does not imply the absence of *SMARCA4* deficiency in tumors of the female reproductive system. In fact, *SMARCA4* loss was first identified in ovarian small-cell carcinoma hypercalcemia type (SCCOHT) as early as 1982 [35]. SCCOHT is a rare aggressive ovarian malignancy associated with hypercalcemia in two-thirds of cases. Unlike most undifferentiated ovarian carcinomas with large cells and abundant cytoplasm, it has small cells [36]. SCCOHT shares similarities with rhabdoid tumors; both show SWI/SNF-complex mutations and poor response to conventional therapy [37]. Cervical *SMARCA4*-UT remains an extremely rare entity, with only limited reports published by the Sirák team [2] and the Yokoe team [3]. The histological features in case report were largely similar to those cases, although minor differences in immunohistochemical profiles were observed (Table 2, Ref. [2,3]). Neither of the previously reported cases demonstrated *SMARCA4* loss in molecular testing, and other molecular features were not fully characterized. The genetic findings presented herein may aid in better defining the molecular landscape of such rare tumors. The published case reports and the present case are comprehensively detailed in Table 2 with respect to the site of symptom onset, histological characteristics, immunohistochemical findings, therapeutic regimens, and prognostic outcomes.

In terms of treatment, surgical resection remains the primary therapeutic strategy for localized disease. In the case reported by Yokoe's team [3], laparoscopic resection was performed with negative margins. Postoperative concurrent chemoradiotherapy (CCRT) was administered at a total dose of 50 Gy in 28 fractions. Weekly cisplatin (40 mg/m^2) was given for six cycles without significant adverse events. Follow-up showed sustained serum carcinoembryonic antigen (CEA) levels below 5.0 ng/mL, and imaging along with vaginal cuff cytology revealed no signs of recurrence at a one-year post-treatment follow-up. However, prognosis tends to be poorer in inoperable cases. The patient reported by Sirák's team [2] received two cycles of cisplatin plus etoposide as first-line therapy after radical hysterectomy was deemed unfeasible. Upon progression, extended pelvic radiotherapy (45 Gy in 25 fractions) was delivered, but the patient succumbed three months later.

In the present case, the large tumor burden precluded radical surgery, prompting treatment with percutaneous radioactive seed implantation (PORT). Subsequent chemotherapy with the etoposide-cisplatin (EP regimen) combined with bevacizumab was initiated. However, significant myelosuppression necessitated a switch to the paclitaxel-carboplatin (TP regimen). Given the MSI-H status detected via NGS, pembrolizumab was added to the treatment protocol. Three months later, imaging revealed tumor progression, leading to a revised regimen of reduced-dose EP chemotherapy with continued bevacizumab. From March 2025 (third discharge) until the latest follow-up, the

Table 2. Comparative analysis of case characteristics.

Case	Age (years)	Location/Initial symptoms	Pathological features	Molecular characteristics	Treatment	Prognosis
Sirák *et al*. [2]	18	Cervix/Abnormal vaginal bleeding	The tumor consists entirely of large cells with vesicular nuclei (rarely hyperchromatic) and often prominent nucleoli. The abundant, eosinophilic cytoplasm sometimes shows rhabdoid morphology. IHC CK(+), MLH1(+), PMS2(+), MSH2(+), MSH6(+), p16(+), p63(–), p40(–), SMARCA4(–).	No other gene variants encoding the SWI/SNF complex were found.	The mass was not resected. Cisplatin plus etoposide was used in combination with extended pelvic radiotherapy.	Three months after the treatment, which was seven months after the initial diagnosis, the patient unfortunately passed away.
Yokoe *et al*. [3]	40	Cervix/Irregular menstruation	Histology shows adenocarcinoma, with visible luminal structures and rhabdoid features, suggesting poorly differentiated malignant tissue. IHC: p16(+), p53, desmin, SOX10, and SMARCA4(–).	Not mentioned.	Surgical resection of the mass, followed by CCRT combined with cisplatin after surgery.	There is no evidence of recurrence more than one year after the completion of CCRT.
Our case	58	Cervix/Persistent vaginal bleeding	A large amount of necrosis is seen within the mass. The tumor cells are large, with rhabdoid features. The cytoplasm is abundant and eosinophilic. A mucoid stroma is observed. IHC: AE1/AE3 is partially positive, p40 (focally +), p16 (patchily +), mismatch repair protein MLH1(–), MSH2(+), MSH6(+), PMS2(–), p53 (90% +), and SMARCA4(–).	Missense mutations in *PTEN*, *PIK3CA*, *MYC*, *BCOR*, *LRP1B*, *ZNRF3*, *NOTCH3*, and *MUC16*; frameshift mutations in *KRAS*, *ARID1A*, and *CFTR*; and an insertion mutation in *CCND1*.	No surgery was performed. After PORT, EP regimen combined with bevacizumab was used for treatment.	The patient's overall condition remains stable, and currently, the patient is in a state of living with the tumor.

CK, cytokeratin; MLH1, MutL homolog 1; PMS2, postmeiotic segregation increased 2; MSH2, MutS homolog 2; MSH6, MutS homolog 6; p16, cyclin-dependent kinase inhibitor 2a; p63, tumor protein p63; p40, Delta N p63; p53, tumor protein p53; SOX10, SRY-box transcription factor 10; CCRT, concurrent chemoradiotherapy; EP regimen, etoposide-cisplatin; PORT, percutaneous radioactive seed implantation.

patient remained clinically stable with tumor-bearing survival. These findings suggested that immunotherapy may offer limited efficacy in inoperable *SMARCA4*-UT, whereas chemotherapy combined with anti-VEGF agents may provide partial tumor growth inhibition.

During this therapeutic intervention, we administered bevacizumab, an anti-VEGF agent. This monoclonal antibody specifically binds to VEGF, thereby blocking its interaction with endothelial cell surface receptors [including fms-like tyrosine kinase 1 (Flt-1) and kinase insert domain receptor (KDR)], which consequently inhibits tumor angiogenesis and restricts malignant proliferation. Notably, investigations of colorectal cancer have demonstrated that *SMARCA4* promotes VEGF-A expression and angiogenesis within tumor microenvironments, suggesting its potential as a therapeutic target [38]. However, this conclusion contradicts our current data. The investigators of that study also acknowledged this discrepancy, attributing it to the context-dependent dual biological functions of *SMARCA4*, which manifests either pro-tumorigenic or anti-tumor effects across distinct cancer types. This mechanistic divergence necessitates further investigation through molecular studies.

4. Conclusions

Cervical *SMARCA4*-UT represents an exceptionally rare and aggressive malignancy. Its low incidence, poorly differentiated morphology, and aggressive clinical behavior pose significant diagnostic and therapeutic challenges. The in-depth analysis of this case facilitated the formulation of more standardized and precise clinical approaches for the management of such rare tumors. Given the rarity of this tumor subtype, the present report constituted an isolated case study lacking large-scale clinical validation. Future multi-center clinical trials with substantial cohorts are warranted to establish therapeutic efficacy for cervical *SMARCA4*-UT, particularly in identifying specific patient subgroups deriving benefit from combined immunotherapy, chemotherapy, and anti-angiogenic agents. The correlation between molecular markers (such as *SMARCA4* deletion status), MSI/mismatch repair (MMR) profiles, concomitant driver-gene alterations, and treatment response is a critical area that requires further investigation. This is evidenced by the significance of MSI/MMR as predictive biomarkers in immunotherapy, to clarify the molecular underpinnings of precision medicine in rare malignancies. Notably, the patient's extended survival with persistent tumor burden demonstrated that sustained disease stabilization through personalized therapy, even without achieving complete remission, can significantly enhance quality of life and provide clinically relevant insights for managing inoperable advanced disease. However, clinical application should refrain from indiscriminately extrapolating individualized regimens due to the inherent limitations of single-case reports. For patients receiving chemotherapy combined with anti-angiogenic therapy, it is imperative to rigorously monitor treatment-related adverse events (e.g., myelosuppression) to ensure therapeutic safety and continuity.

Availability of Data and Materials

The datasets used and analyzed during the current study are available from the corresponding author on reasonable request.

Author Contributions

JW and CL main authors of manuscript, have made substantial contributions to conception and design of study, acquisition of data, drafting of the manuscript and critical revision of the manuscript, YL designed the study and acquired pathological data; WD acquired clinical data. All authors contributed to critical revision of the manuscript for important intellectual content. All authors read and approved the final manuscript. All authors have participated sufficiently in the work and agreed to be accountable for all aspects of the work.

Ethics Approval and Consent to Participate

The study was carried out in accordance with the guidelines of the Declaration of Helsinki and was approved by the Ethics Committee of Ruijin Hospital, affiliated with Shanghai Jiao Tong University School of Medicine. Written informed consent was obtained from both the patient and her immediate family members for the publication of this clinical case report.

Acknowledgment

Not applicable.

Funding

This research received no external funding.

Conflict of Interest

The authors declare no conflict of interest.

Supplementary Material

Supplementary material associated with this article can be found, in the online version, at https://doi.org/10.31083/CEOG45103.

References

[1] Nambirajan A, Jain D. Recent updates in thoracic SMARCA4-deficient undifferentiated tumor. Seminars in Diagnostic Pathology. 2021; 38: 83–89. https://doi.org/10.1053/j.semdp.2021.06.001.

[2] Sirák I, Laco J, Vošmiková H, Mell LK, Herrera FG, Šenkeříková M, *et al*. SMARCA4-Deficient Carcinoma of Uterine Cervix Resembling SCCOHT-Case Report. Pathology Oncology Research: POR. 2021; 27: 1610003. https://doi.org/10.3389/pore.2021.1610003.

[3] Yokoe T, Oku K, Noda Y, Kita M. Treatment for SMARCA4-deficient carcinoma of uterine cervix. BMJ Case Reports. 2025; 18: e258711. https://doi.org/10.1136/bcr-2023-258711.

[4] Kolin DL, Quick CM, Dong F, Fletcher CDM, Stewart CJR, Soma A, *et al*. SMARCA4-deficient Uterine Sarcoma and Undifferentiated Endometrial Carcinoma Are Distinct Clinicopathologic Entities. The American Journal of Surgical Pathology. 2020; 44: 263–270. https://doi.org/10.1097/PAS.0000000000001375.

[5] Medina PP, Sanchez-Cespedes M. Involvement of the chromatin-remodeling factor BRG1/SMARCA4 in human cancer. Epigenetics. 2008; 3: 64–68. https://doi.org/10.4161/epi.3.2.6153.

[6] Stanton BZ, Hodges C, Calarco JP, Braun SMG, Ku WL, Kadoch C, *et al*. Smarca4 ATPase mutations disrupt direct eviction of PRC1 from chromatin. Nature Genetics. 2017; 49: 282–288. https://doi.org/10.1038/ng.3735.

[7] Lissanu Deribe Y, Sun Y, Terranova C, Khan F, Martinez-Ledesma J, Gay J, *et al*. Mutations in the SWI/SNF complex induce a targetable dependence on oxidative phosphorylation in lung cancer. Nature Medicine. 2018; 24: 1047–1057. https://doi.org/10.1038/s41591-018-0019-5.

[8] Kadoch C, Crabtree GR. Mammalian SWI/SNF chromatin remodeling complexes and cancer: Mechanistic insights gained from human genomics. Science Advances. 2015; 1: e1500447. https://doi.org/10.1126/sciadv.1500447.

[9] Fernando TM, Piskol R, Bainer R, Sokol ES, Trabucco SE, Zhang Q, *et al*. Functional characterization of SMARCA4 variants identified by targeted exome-sequencing of 131,668 cancer patients. Nature Communications. 2020; 11: 5551. https://doi.org/10.1038/s41467-020-19402-8.

[10] Dagogo-Jack I, Schrock AB, Kem M, Jessop N, Lee J, Ali SM, *et al*. Clinicopathologic Characteristics of BRG1-Deficient NSCLC. Journal of Thoracic Oncology. 2020; 15: 766–776. https://doi.org/10.1016/j.jtho.2020.01.002.

[11] La Fleur L, Falk-Sörqvist E, Smeds P, Berglund A, Sundström M, Mattsson JS, *et al*. Mutation patterns in a population-based non-small cell lung cancer cohort and prognostic impact of concomitant mutations in KRAS and TP53 or STK11. Lung Cancer. 2019; 130: 50–58. https://doi.org/10.1016/j.lungcan.2019.01.003.

[12] Schoenfeld AJ, Bandlamudi C, Lavery JA, Montecalvo J, Namakydoust A, Rizvi H, *et al*. The Genomic Landscape of *SMARCA4* Alterations and Associations with Outcomes in Patients with Lung Cancer. Clinical Cancer Research. 2020; 26: 5701–5708. https://doi.org/10.1158/1078-0432.CCR-20-1825.

[13] Xue Y, Morris JL, Yang K, Fu Z, Zhu X, Johnson F, *et al*. SMARCA4/2 loss inhibits chemotherapy-induced apoptosis by restricting IP3R3-mediated Ca^{2+} flux to mitochondria. Nature Communications. 2021; 12: 5404. https://doi.org/10.1038/s41467-021-25260-9.

[14] Berlin M, Cantley J, Bookbinder M, Bortolon E, Broccatelli F, Cadelina G, *et al*. PROTACs Targeting BRM (SMARCA2) Afford Selective *In Vivo* Degradation over BRG1 (SMARCA4) and Are Active in BRG1 Mutant Xenograft Tumor Models. Journal of Medicinal Chemistry. 2024; 67: 1262–1313. https://doi.org/10.1021/acs.jmedchem.3c01781.

[15] Nicholson AG, Tsao MS, Beasley MB, Borczuk AC, Brambilla E, Cooper WA, *et al*. The 2021 WHO Classification of Lung Tumors: Impact of Advances Since 2015. Journal of Thoracic Oncology. 2022; 17: 362–387. https://doi.org/10.1016/j.jtho.2021.11.003.

[16] Xiong Y, Zhang B, Nie LG, Wu SK, Zhao H, Li D, *et al*. Thoracic *SMARCA4*-deficient undifferentiated tumor-pathological diagnosis and combined immune checkpoint inhibitor treatment. Journal of Peking University. Health Sciences. 2023; 55: 351–356. https://doi.org/10.19723/j.issn.1671-167X.2023.02.022.

[17] He S, Wu Z, Tian Y, Yu Z, Yu J, Wang X, *et al*. Structure of nucleosome-bound human BAF complex. Science. 2020; 367: 875–881. https://doi.org/10.1126/science.aaz9761.

[18] Jiménez C, Antonelli R, Nadal-Ribelles M, Devis-Jauregui L, Latorre P, Solé C, *et al*. Structural disruption of BAF chromatin remodeller impairs neuroblastoma metastasis by reverting an invasiveness epigenomic program. Molecular Cancer. 2022; 21: 175. https://doi.org/10.1186/s12943-022-01643-4.

[19] Chang L, Azzolin L, Di Biagio D, Zanconato F, Battilana G, Lucon Xiccato R, *et al*. The SWI/SNF complex is a mechanoregulated inhibitor of YAP and TAZ. Nature. 2018; 563: 265–269. https://doi.org/10.1038/s41586-018-0658-1.

[20] Hao F, Zhang Y, Hou J, Zhao B. Chromatin remodeling and cancer: the critical influence of the SWI/SNF complex. Epigenetics & Chromatin. 2025; 18: 22. https://doi.org/10.1186/s13072-025-00590-w.

[21] Le Loarer F, Watson S, Pierron G, de Montpreville VT, Ballet S, Firmin N, *et al*. SMARCA4 inactivation defines a group of undifferentiated thoracic malignancies transcriptionally related to BAF-deficient sarcomas. Nature Genetics. 2015; 47: 1200–1205. https://doi.org/10.1038/ng.3399.

[22] Rekhtman N, Montecalvo J, Chang JC, Alex D, Ptashkin RN, Ai N, *et al*. SMARCA4-Deficient Thoracic Sarcomatoid Tumors Represent Primarily Smoking-Related Undifferentiated Carcinomas Rather Than Primary Thoracic Sarcomas. Journal of Thoracic Oncology. 2020; 15: 231–247. https://doi.org/10.1016/j.jtho.2019.10.023.

[23] World Health Organization (WHO). Thoracic Tumors. International Agency for Research on Cancer: Lyon. 2021.

[24] Liang X, Gao X, Wang F, Li S, Zhou Y, Guo P, *et al*. Clinical characteristics and prognostic analysis of SMARCA4-deficient non-small cell lung cancer. Cancer Medicine. 2023; 12: 14171–14182. https://doi.org/10.1002/cam4.6083.

[25] Ma X, Long X, Song F, Lv J. SMARCA4-Deficient Undifferentiated Gallbladder Cancer: A Case Report and Review of the Literature. International Journal of Surgical Pathology. 2025; 33: 1057–1061. https://doi.org/10.1177/10668969241297259.

[26] Kakkar A, Ashraf SF, Rathor A, Adhya AK, Mani S, Sikka K, *et al*. SMARCA4/BRG1-Deficient Sinonasal Carcinoma. Archives of Pathology & Laboratory Medicine. 2022; 146: 1122–1130. https://doi.org/10.5858/arpa.2021-0001-OA.

[27] Shi M, Chen X, Liu T, Yin S, Lin Z. SMARCA4 deficient undifferentiated tumor in nasopharynx. Oral Oncology. 2025; 161: 107162. https://doi.org/10.1016/j.oraloncology.2024.107162.

[28] Shweikeh F, Hong G, Walter J, Hoscheit M, Lembo A, Mouchli M, *et al*. SMARCA4-Deficient Undifferentiated Esophageal Carcinoma: A Clinical Case Series and Literature Review. Journal of Gastrointestinal Cancer. 2024; 55: 1433–1440. https://doi.org/10.1007/s12029-024-01060-4.

[29] Deng L, Li B. A case report of SMARCA4-deficient undifferentiated tumor in the esophago-gastric junction. Asian Journal of Surgery. 2023; 46: 5330–5331. https://doi.org/10.1016/j.asjsur.2023.07.078.

[30] An HR, Kim HD, Ryu MH, Park YS. SMARCA4-deficient undifferentiated gastric carcinoma: a case series and literature review. Gastric Cancer. 2024; 27: 1147–1152. https://doi.org/10.1007/s10120-024-01510-9.

[31] Kambe A, Yamamoto Y, Hasegawa C, Kakiuchi A, Kojima D, Hino A, *et al*. SMARCA4-deficient tumors in the adrenal gland and small intestines: A rare case report. Radiology Case Reports. 2023; 19: 794–797. https://doi.org/10.1016/j.radcr.2023.11.038.

[32] Arihara Y, Omori G, Kobayashi K, Sugita S, Murase K, Kubo T, *et al*. Marked Response to Nivolumab by a Patient With SMARCA4-Deficient Undifferentiated Urothelial Carcinoma

Showing High PD-L1 Expression: A Case Report. Cancer Reports. 2024; 7: e2127. https://doi.org/10.1002/cnr2.2127.
[33] Gumusgoz E, Graham BS, Hosler GA. Primary cutaneous SMARCA4-deficient undifferentiated malignant neoplasm: A rare case report and literature review. Journal of Cutaneous Pathology. 2024; 51: 262–266. https://doi.org/10.1111/cup.14576.
[34] Höhn AK, Brambs CE, Hiller GGR, May D, Schmoeckel E, Horn LC. 2020 WHO Classification of Female Genital Tumors. Geburtshilfe Und Frauenheilkunde. 2021; 81: 1145–1153. https://doi.org/10.1055/a-1545-4279.
[35] Dickersin GR, Kline IW, Scully RE. Small cell carcinoma of the ovary with hypercalcemia: a report of eleven cases. Cancer. 1982; 49: 188–197. https://doi.org/10.1002/1097-0142(19820101)49:1<188::aid-cncr2820490137>3.0.co;2-d.
[36] Young RH, Goodman A, Penson RT, Russell AH, Uppot RN, Tambouret RH. Case records of the Massachusetts General Hospital. Case 8-2010. A 22-year-old woman with hypercalcemia and a pelvic mass. The New England Journal of Medicine. 2010; 362: 1031–1040. https://doi.org/10.1056/NEJMcpc1000272.
[37] Brennan B, Stiller C, Bourdeaut F. Extracranial rhabdoid tumours: what we have learned so far and future directions. The Lancet. Oncology. 2013; 14: e329–36. https://doi.org/10.1016/S1470-2045(13)70088-3.
[38] Lan J, Li H, Luo X, Hu J, Wang G. BRG1 promotes VEGF-A expression and angiogenesis in human colorectal cancer cells. Experimental Cell Research. 2017; 360: 236–242. https://doi.org/10.1016/j.yexcr.2017.09.013.